EXTENSIONAL VISCOSITY OF HIGHLY ALIGNED DISCONTINUOUS FIBER 'TuFF' COMPOSITES IN STRETCH FORMING PROCESSES

UNIVERSITY OF DELAWARE | CENTER FOR COMPOSITE MATERIALS

Henry Fidlow[1,2], Dr. Thomas A. Cender[1], Dr. Pavel Simacek[1,2], Prof. Suresh G. Advani[1,2]
University of Delaware | Center for Composite Materials[1] | Department of Mechanical Engineering[2]

Introduction

TuFF is a highly-aligned, short fiber composite with fiber volume fractions close to 60%. The high fiber to polymer ratio yields impressive mechanical properties while the use of short fibers can allow for cheap, environmentally-friendly manufacturing as a result of fiber recyclability. Although TuFF is unidirectionally anisotropic at the ply-scale, combining plies in alternating orientations (0º, ±45º, 90º) produces quasi-isotropic properties. Unlike most long fiber and continuous fiber composites, fiber suspension in the polymer enables stretching in the fiber direction due to polymer shear. This behavior allows for the design and production of shapes more complex than can otherwise be made using existing composite technologies.

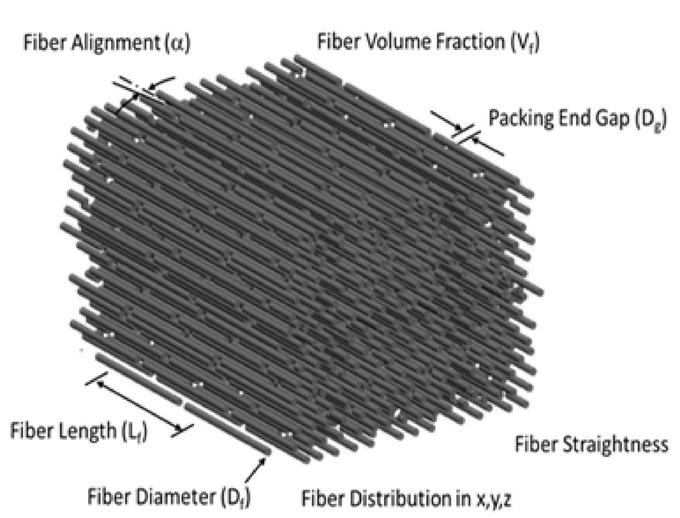

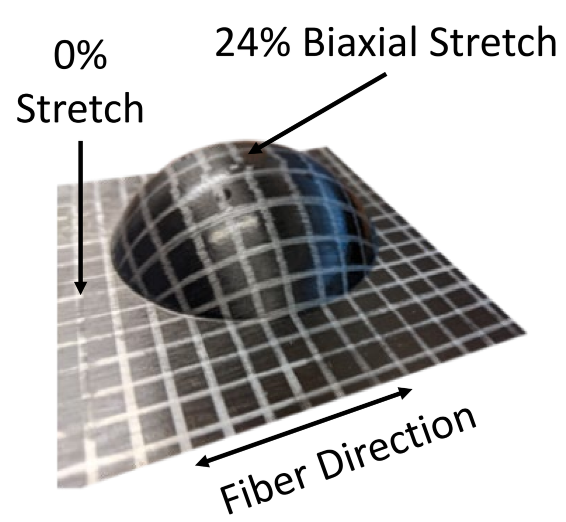

Project Objectives:

Characterize the directional stretching behavior of TuFF to develop material constitutive laws from stress, strain, strain rate, and temperature. Constitutive laws will be implemented in new a finite element material forming simulation for TuFF composite forming.

Problem Specification

Investigate ply-scale anisotropic viscosity in the 0º direction of TuFF by applying uniaxial tension in the fiber direction.

Impart environmental controls to determine temperature and strain rate dependence.

$$\begin{bmatrix}\sigma_1\\ \sigma_2\\ \sigma_6\end{bmatrix} = \begin{bmatrix}\eta_{11} & \eta_{12} & 0\\ \eta_{12} & \eta_{22} & 0\\ 0 & 0 & \eta_{66}\end{bmatrix}\begin{bmatrix}\dot{\varepsilon}_1\\ \dot{\varepsilon}_2\\ \dot{\varepsilon}_6\end{bmatrix}$$

$T = const.$
$\dot{\varepsilon} = const.$

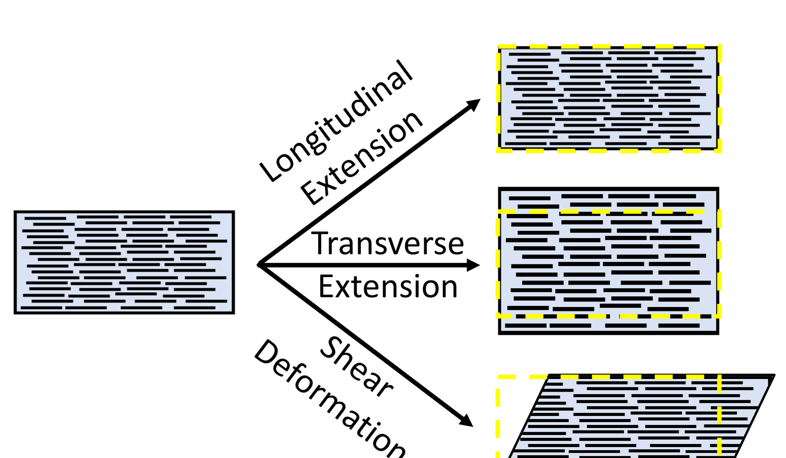

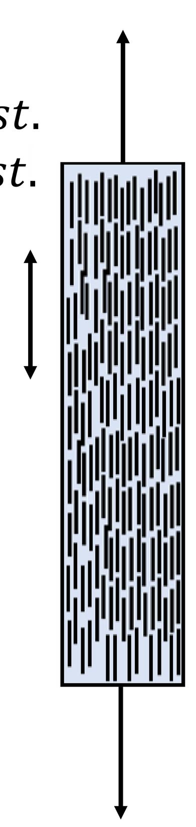

$\eta_{11} \approx \frac{\sigma_1}{\dot{\varepsilon}_1}$

$\eta_{22} \approx \frac{\sigma_2}{\dot{\varepsilon}_2}$

Methodology

Prior to Testing:

- Manufacture CF-PEI TuFF blanks and cut out 0º samples for testing
- Speckle samples to obtain surface strain data during testing using digital image correlation (DIC)
- Measure undeformed sample dimensions

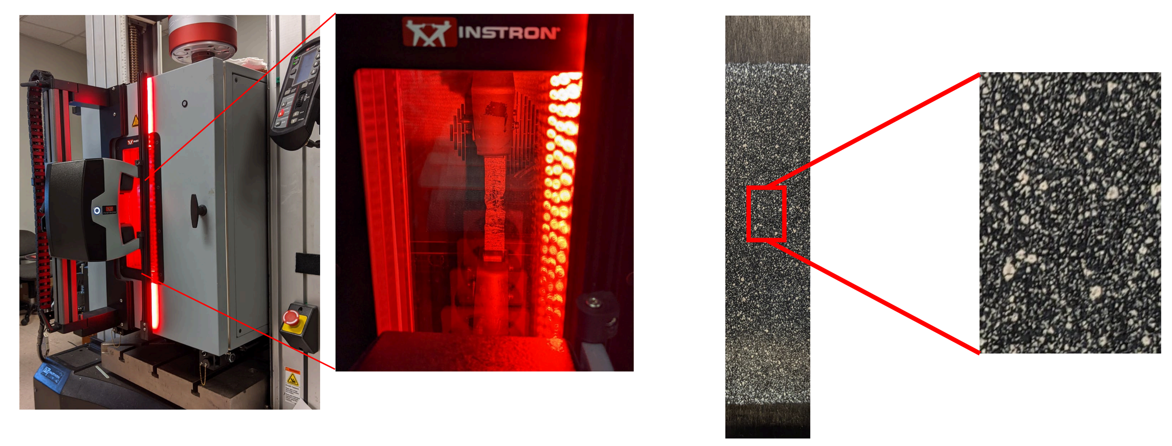

During Testing:

- Heat sample to melt and hold isothermally
- Load sample in uniaxial tension
- Apply constant true strain rate until 10% strain is reached and allow sample stress to relax
- Obtain time, force, and displacement from Instron
- Use video extensometer to observe deformation of speckle pattern

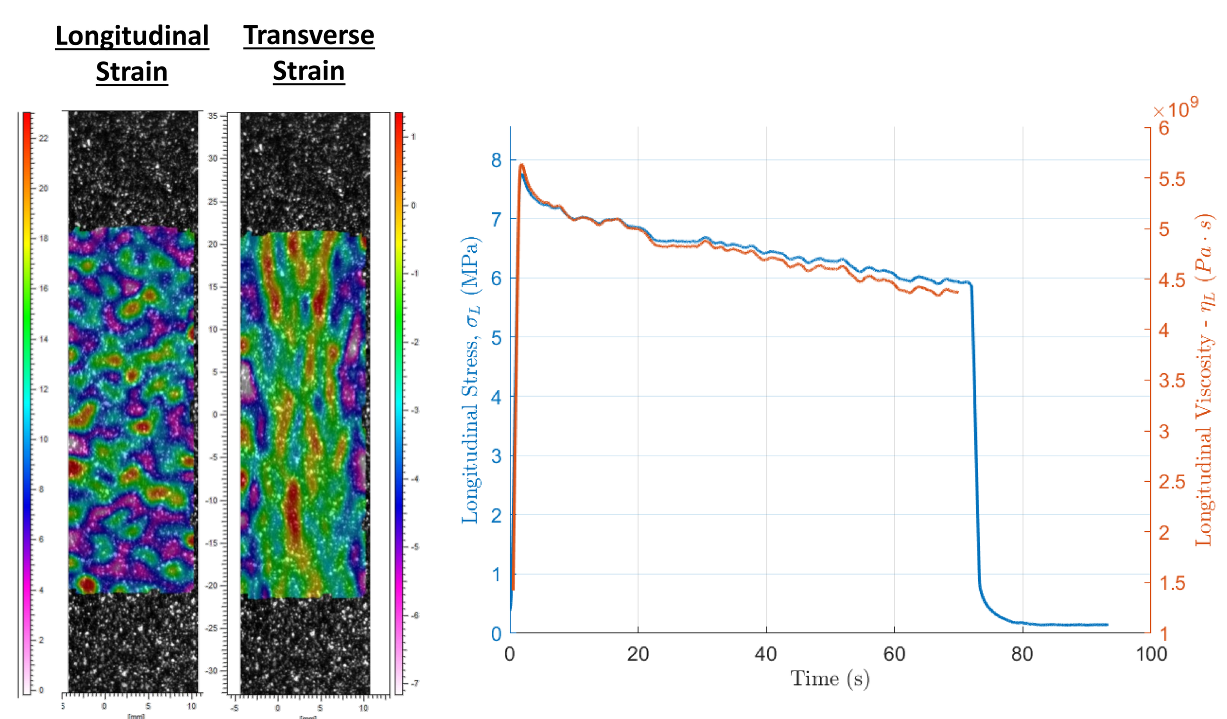

Data Analysis using DIC:

- Set the undeformed image as the reference
- Use time data along with DIC algorithm to find the local and average surface strain (axial and transverse) along the gauge section
- Assuming composite incompressibility (neglecting porous volume), determine the true stress of the sample with respect to axial strain
- Calculate viscosity and average strain rate within the sample gauge section

Results and Discussion

Strain Dependence:

At 330°C, various strain-rates were evaluated. Stress remained relatively constant with strain but strain-rate effect was large.

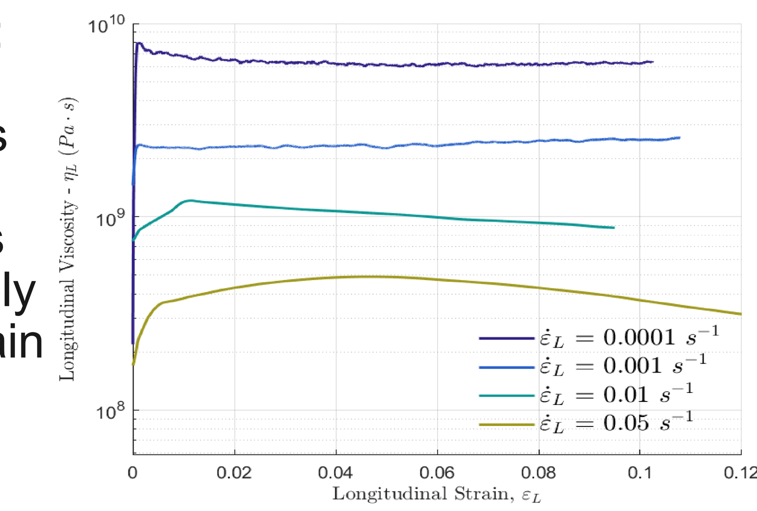

Strain Uniformity:

- At different average strains, the distribution of local strain values can be calculated to show deviation from the mean
- Areas of high local strain can be used to predict the location of initial failure at high average strain

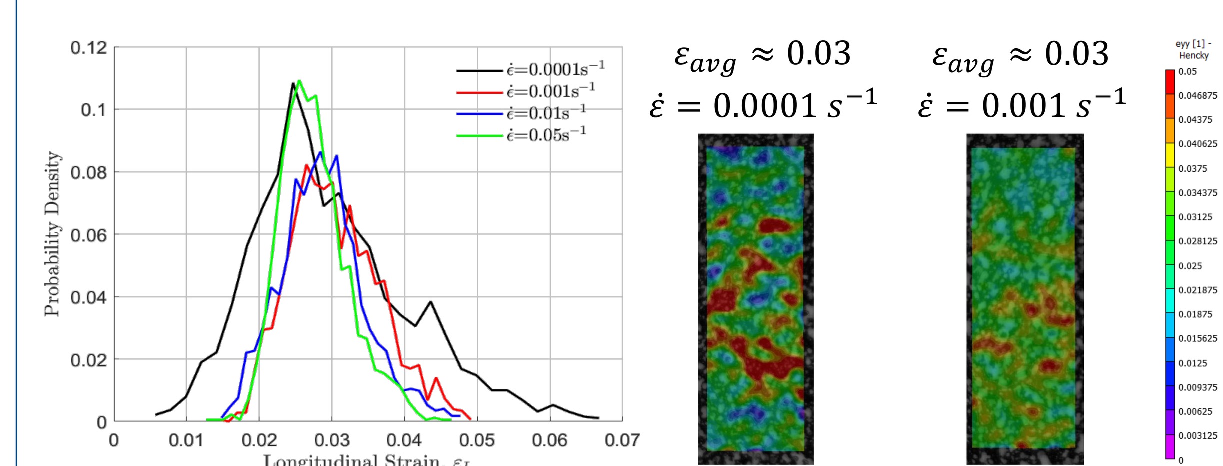

Power-law Fluid:

- Viscosity decreases with increasing strain rate, indicating shear thinning behavior

$\sigma_1 = K\dot{\varepsilon}_1^{\,n}$ or $\eta_{11} = K\dot{\varepsilon}_1^{\,n-1}$ $\quad K(T) = Ae^{E/RT}$

$n \approx 0.632 \quad A \approx 4.83 \cdot 10^{-5}\ Pa * s^n \quad E \approx 147\ kJ/mol$

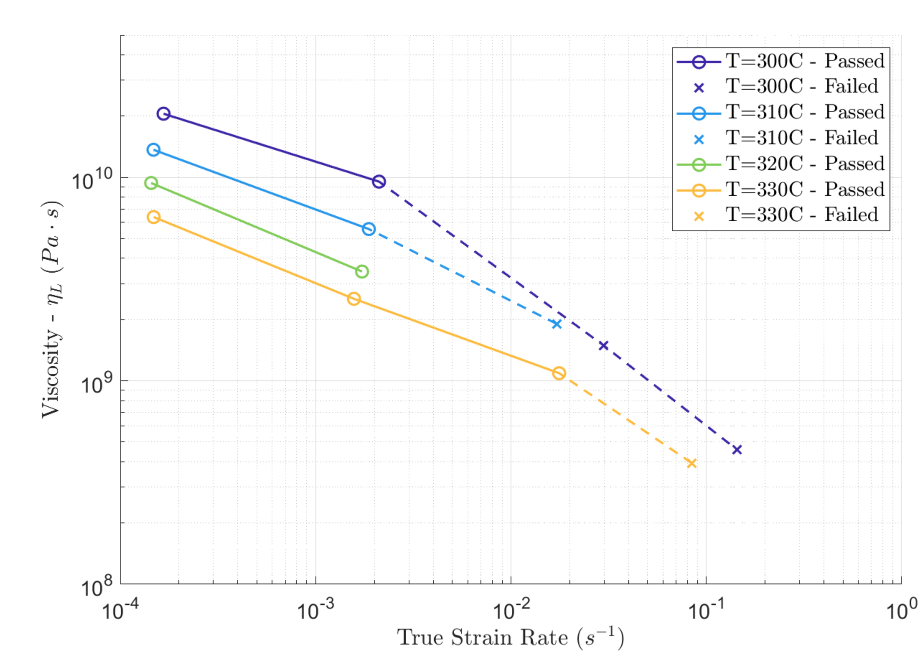

Shear Magnification:

- Large aspect ratios in the fibers result in a large shear rate to strain rate ratio

$\dot{\varepsilon} = 0.0001\ s^{-1} \longrightarrow \dot{\varepsilon} = 0.1\ s^{-1}$

$\dot{\gamma} = 0.2\ s^{-1} \longrightarrow \dot{\gamma} = 200\ s^{-1}$

$$\frac{\dot{\gamma}}{\dot{\varepsilon}_1} = \frac{2}{\ln\sqrt{V_f}}\frac{L}{D} \approx 2 \times 10^3$$

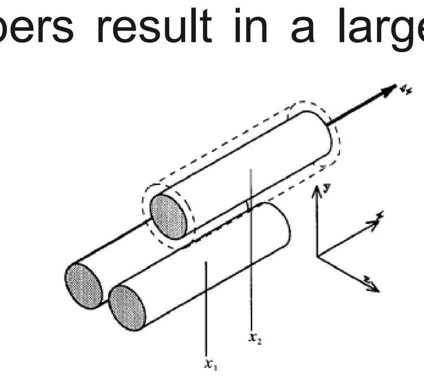

Creasy & Advani J. *Non-Newt. Fluid Mech. 73* (1997)

Summary and Conclusion

Viscosity Observations:

- Viscosity had a low dependence on strain, indicating that microstructural changes (due to stretching) were small enough to have little influence on the stress response
- Viscosity exhibited a logarithmic dependance with strain rate and temperature—which is consistent with the expected polymer viscosity behavior

Fluid Modelling:

- The relationship between average viscosity and strain rate was well characterized as a shear thinning fluid, which was captured by a power law model
- Shear thinning behavior, which occurs in polymers at high strain rate, can be explained by shear magnification; the large shear rate in the polymer is a result of fiber spacing and aspect ratios

Surface Strain Behavior:

- Surface strain can be used to predict locations of failure as well as deformation of the microstructure

The goal of this project was to determine the anisotropic viscosity of TuFF in the fiber direction such that we could apply this value to a material forming model. On this front, we successfully found a relationship between η_{11}, T, and $\dot{\varepsilon}_1$. The strain independence allowed us to fit a power law model to the η_{11} vs. $\dot{\varepsilon}_1$ curve to obtain the flow consistency index, K, and power law index, n. Given that $0 < n < 1$, we observed shear thinning behavior which can be explained through shear magnification. Due to the temperature dependence of K, we were able to fit the Arrhenius equation to our system to find the pre-exponential factor, A, and the activation energy, E. Testing will continue to be conducted to obtain more data for fitting parameters. Additional investigation will be conducted to determine transverse behavior and the effects of local strain distributions.

Acknowledgements

This material is based upon work supported by the National Aeronautics and Space Administration under Grant and Cooperative Agreement No. 80NSSC20M0164, issued through the Aeronautics Research Mission Directorate, Transformative Aeronautics Concepts Program, University Leadership Initiative.

Co-Sponsored by:
University Leadership Initiative (ULI)

Partner